

# Swelling, softening, and elastocapillary adhesion of cooked pasta


Cite as: Phys. Fluids **34**, 042105 (2022); <https://doi.org/10.1063/5.0083696>

Submitted: 29 December 2021 • Accepted: 04 March 2022 • Published Online: 04 April 2022

 Jonghyun Hwang,  Jonghyun Ha,  Ryan Siu, et al.

## COLLECTIONS

Paper published as part of the special topic on [Kitchen Flows](#)

 This paper was selected as Featured



View Online



Export Citation



CrossMark

## ARTICLES YOU MAY BE INTERESTED IN

[Rheology-driven design of pizza gas foaming](#)

Physics of Fluids **34**, 033109 (2022); <https://doi.org/10.1063/5.0081038>

[Black tea interfacial rheology and calcium carbonate](#)

Physics of Fluids **33**, 092105 (2021); <https://doi.org/10.1063/5.0059760>

[Contribution of flow topology to the kinetic energy flux in hypersonic turbulent boundary layer](#)

Physics of Fluids **34**, 046103 (2022); <https://doi.org/10.1063/5.0089126>

APL Machine Learning

Open, quality research for the networking communities

OPEN FOR SUBMISSIONS MAY 2022

LEARN MORE



# Swelling, softening, and elastocapillary adhesion of cooked pasta

Cite as: Phys. Fluids **34**, 042105 (2022); doi: [10.1063/5.0083696](https://doi.org/10.1063/5.0083696)

Submitted: 29 December 2021 · Accepted: 4 March 2022 ·

Published Online: 4 April 2022



View Online



Export Citation



CrossMark

Jonghyun Hwang,<sup>1</sup>  Jonghyun Ha,<sup>1</sup>  Ryan Siu,<sup>1</sup>  Yun Seong Kim,<sup>1,2</sup>  and Sameh Tawfik<sup>1,2,a)</sup> 

## AFFILIATIONS

<sup>1</sup>Department of Mechanical Science and Engineering, University of Illinois at Urbana-Champaign, Urbana, Illinois 61801, USA

<sup>2</sup>The Beckman Institute for Advanced Science and Technology, University of Illinois at Urbana-Champaign, Urbana, Illinois 61801, USA

Note: This paper is part of the special topic, Kitchen Flows.

<sup>a)</sup>Author to whom correspondence should be addressed: [tawfik@illinois.edu](mailto:tawfik@illinois.edu)

## ABSTRACT

The diverse chemical and physical reactions encountered during cooking connect us to science every day. Here, we theoretically and experimentally investigate the swelling and softening of pasta due to liquid imbibition as well as the elastic deformation and adhesion of pasta due to capillary force. As water diffuses into the pasta during cooking, it softens gradually from the outside inward as starch swells and relaxes. The softening follows three sequential regimes: regime I, the hard-glassy region, shows a slow decrease in modulus with cooking time; regime II, the glassy to rubbery transition region, or leathery region, is characterized by a very fast, several orders of magnitude drop in elastic modulus and regime III, the rubbery region, has an asymptotic modulus about four orders of magnitude lower than the raw pasta. We present experiments and theory to capture these regimes and relate them to the heterogeneous microstructure changes associated with swelling. Interestingly, we observe a modulus drop of two orders of magnitude within the range of “al dente” cooking duration, and we find the modulus to be extremely sensitive to the amount of salt added to the boiling water. While most chefs can gauge the pasta by tasting its texture, our proposed experiment, which only requires a measurement with a ruler, can precisely provide an optimal cooking time finely tuned for various kinds of pasta shapes.

Published under an exclusive license by AIP Publishing. <https://doi.org/10.1063/5.0083696>

Pasta cooking offers intriguing chemo-mechanical and hydrostatic and -dynamic phenomena for the curious mind.<sup>1–3</sup> Examples of such phenomena manifest themselves due to interaction between soft elastic solids and liquid such as in steaming dumplings, frying potatoes, and swelling of noodles. Liquid and heat transport into cooked media can change the materials' shape and mechanical properties.<sup>3–6</sup> Another common example is seen with starch, the most abundant carbohydrate in human diets, which expands and softens as it experiences hygroscopic swelling.<sup>7–9</sup> In addition to swelling, capillary attraction and adhesion are commonly encountered during cooking of slender forms like noodles as well as during serving and eating of noodle soups. Complex mechanics laws govern the interactions between fully cooked noodles hanging from a fork and determine how they stick together or fall back down (hopefully) into the bowl.

In this article, we document how pasta, composed of starch granules,<sup>10,11</sup> swells and softens as a function of the cooking duration, water temperature, and the addition of salt. As expected, noodles not only experience volumetric expansion but also their bending rigidity

(elastic modulus multiplied by second moment of area) significantly decrease so that noodles become edible. We focus on a simple but insightful kitchen experiment wherein softened pasta noodles coalesce when the noodle strings are lifted, as demonstrated in Fig. 1(a). The coalescence depicted in the figure is mainly due to increased flexibility. Figure 1(b) shows the time evaluation of hygroscopic swelling of the pasta noodle. Notably, there is a significant increase in length as well. The diameter to length relative swelling anisotropy is 3.5. We break the cooked noodles at various cooking times to observe the cross section. As it is cooked, the raw pasta soon become composed of hard inner regions and softened, cooked outer layers (traditionally expected structure of Al Dente). This soft to hard transition in the radial direction of pasta can be explained by water transport and diffusion starting from the outermost surface of the noodle, hence, the softening initiates from the outermost region. It then reaches the saturation stages, where we observe no color gradient in the cross section (fully soft and arguably overcooked). To study the elasticity of cooked pasta, we solve the liquid diffusion equation to obtain an expression for the concentration

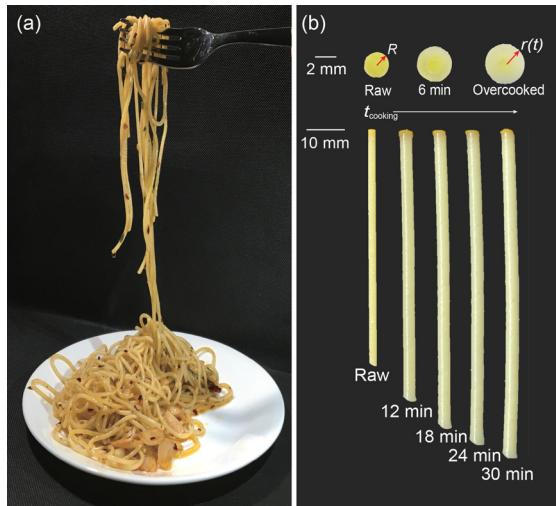


**FIG. 1.** (a) Picture of spaghetti aglio e olio. Capillary adhesion between the noodles is induced by olive oil seasoned with garlic and pepper. (b) Pasta radial and axial growth over time at 100 °C cooking due to hygroscopic swelling. Radial strain grows up to 70% of its original and axial strain up to 40% of its original after 30 min of cooking (at 100 °C). Pasta cross section shows color-gradient before it is sufficiently cooked.

of liquid within the pasta and use it to develop the theoretical model of the swelling dynamics of starch materials. The concentration profile is also used to model the elastic modulus  $E$  of the material based on the pioneering work of Weibull.<sup>12</sup> Combining the two perspectives, swelling and softening, we construct a predictive model for pasta

elastocapillarity, namely, the stick length of the noodles due to capillary forces.<sup>13–21</sup> Overall, we believe that not only is this one of the first studies combining swelling dynamics with elastocapillarity, but also this kitchen experiment is insightful for understanding pasta cooking and for teaching mechanics.

Before turning to the swelling dynamics of pasta, we physically explain the capillary-driven deformation of slender structures, termed elastocapillarity.<sup>16</sup> When slender structures such as thin rods or plates are pulled out of a liquid container, the liquid surface energy causes coalescence. Figure 2 shows the elastocapillary adhesion of two noodles seen during the experiment [Fig. 2(a)] and the schematic representation of the phenomenon [Fig. 2(b)]. A liquid meniscus forms between the coalesced structure [see inset (i) of Fig. 2(b)], and this capillary contact balances the elastic resistance created by the bending of the elastic rods. The adhesion energy created by the surface tension of liquid can be expressed as  $E_c \sim \gamma p(l_0 - l_s)$ , where  $\gamma$ ,  $p$ ,  $l_0$ , and  $l_s$  are the surface tension, perimeter of the wetted surface, length of the noodle, and the stick length [see inset (ii) of Fig. 2(b)], respectively. If the rods are displaced by a distance  $d$ , as shown in Fig. 2(a), the elastic resistance energy to the surface tension can be expressed as  $U_e \sim EI d^2 / l_s^3$ , where  $E$  and  $I$  are the Young’s modulus and the second moment of area, respectively. The stick length is defined as the distance between the fixture and point where the meniscus between the pasta forms.<sup>15,16</sup> Then, an expression for the stick length can be obtained by balancing the two forces,  $F_c$  and  $F_e$ :  $l_s \sim (dl_{ec})^{1/2}$ , where  $l_{ec} = [EI/(\gamma p)]^{1/2}$  is the elastocapillary length.<sup>14,20–22</sup> Since the Young’s modulus,  $E$ , and other geometrical parameters ( $I$  and  $p$ ) vary over time and the surface tension  $\gamma$  is a function of temperature,<sup>23</sup>  $l_{ec}$  is a function of temperature, cooking time, and added salt as described below.

We now move onto finding an expression for the time-variant geometry of the pasta, specifically the  $l/p$  ratio used in the expression

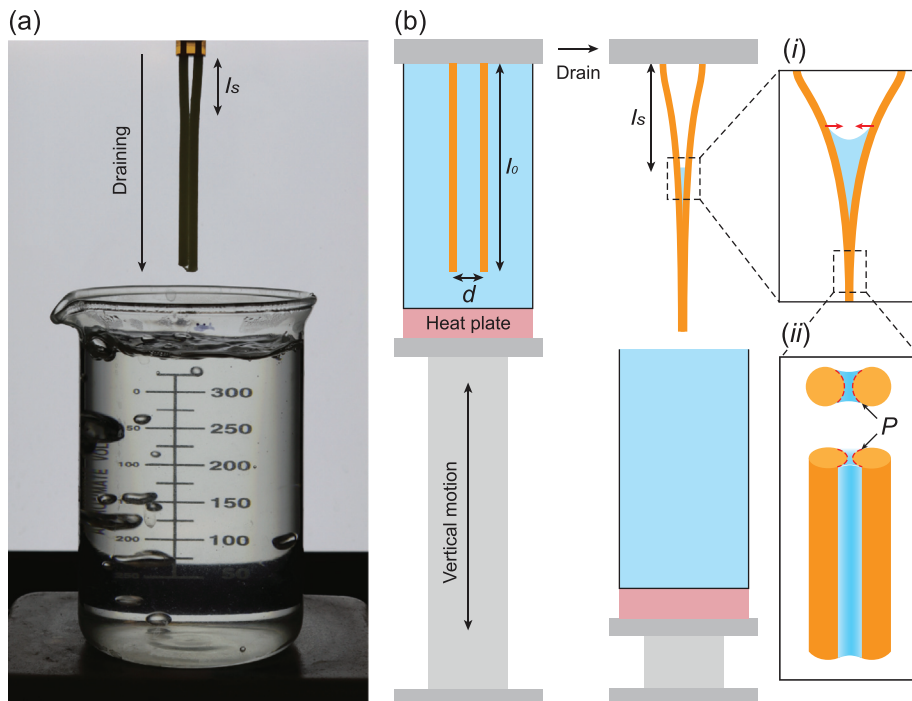


**FIG. 2.** Stick length measurement (a) proposed experimental setup for indirectly inferring the cooked pasta texture, for instance, al dente, by measuring the stick length. Noodle stiction occurs as the linear stage moves down the beaker. (b) Capillary adhesion mechanism analysis. Two pasta noodles displaced by a gap  $d$  and cooked for every 3 min stick to each other when drained if the capillary force is greater than the elastic restoring force. (i) The liquid meniscus that forms between the noodles causes capillary adhesion. (ii) Pasta wetting seen from the axial and transverse directions. We assume the liquid wets each half of the cylinder.

of  $l_{ec}$  and which is strongly affected by the swelling. The radial expansion of the pasta is due to hygroscopic swelling, where migration of the water molecule into the pasta induces expansion of the starch matrix, as represented in Fig. 3(a). To capture how the geometrical factors change over time and their effect on the elastocapillary length, we define a length scale of the cross section of pasta,  $\delta$ . Then, hygroscopically swelled  $\delta$  can be written as  $\delta \sim \delta_0 (1 + \epsilon)$ , where  $\delta_0$  is an initial length scale and  $\epsilon$  is the strain. In the hygroscopically swelling material, we assume that the expansion in volume is entirely due to the radial liquid migration into the material.<sup>24,25</sup> Hence, we solve the diffusion equation to relate the liquid concentration,  $C$ , to the volumetric strain. The diffusion equation with concentration dependent diffusivity,  $D(C)$ , is written as the following:  $\nabla \cdot [D(C)\nabla C] = \partial C/\partial t$ , where the operator  $\nabla$  represents the gradient of our scalar field,  $C$ . Note that the form of Fick's second law used here allows the use of the concentration dependent diffusivity, which can be expressed as Eq. (1) (see Note S1 for the detailed derivation),<sup>26–28</sup>

$$D(C) = D_0 \frac{C}{(1 - C)^{1.5}}, \quad (1)$$

where  $D_0$  is the diffusivity scaling parameter of the material. Considering the initial and boundary conditions, we can numerically solve the nonlinear diffusion equation. The water diffusion into the polymer matrix follows two distinct stages. In the first stage, the concentration reaches  $C^*$  due to diffusion, and in the second stage, it gradually further increases beyond  $C^*$  due to polymer relaxation until it reaches an equilibrium concentration  $C_{EQ} > C^*$ .<sup>29,30,33,34</sup> Then, the dynamics of liquid concentration  $C(r, t)$  leads to the hygroscopic strain in the radial direction, as follows:

$$\epsilon_{rr}(t) \approx \frac{1}{2} \alpha \left[ \frac{V(t) - V_0}{V_0} \right], \quad (2)$$

where  $\alpha$  is the coefficient of radial expansion and  $V_0$  is the initial volume. The amount of liquid absorbed,  $V(t)$ , is governed by the liquid concentration as well as characteristic swelling timescale associated

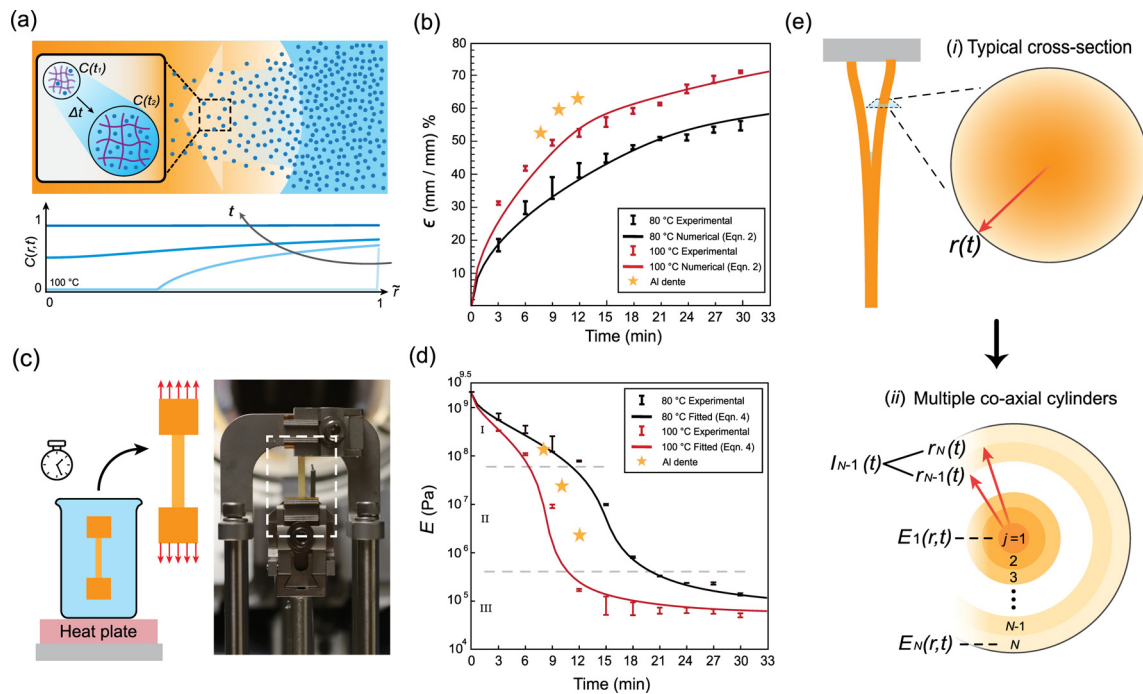


**FIG. 3.** (a) Qualitative description of hygroscopic swelling of pasta. The polymer matrix inside the pasta swells as liquid concentration within the material increases. The swelling is entirely due to the volume of liquid uptaken. Blue dots represent water molecules inside the macromolecular chain.  $C(r, t)$  stands for local concentration. Qualitative depiction of liquid concentration within pasta noodle cooked at 100 °C is provided.  $\bar{r}$  represents normalized radial position. The clockwise arrow labeled “ $t$ ” indicates that curves are drawn in increasing time order (0 min the lightest, 3 min, 10 min, and the 30 min cooking as the darkest). (b) Experimentally measured radial strain data and analytical solution for the radius over time. The coefficient of expansion is  $\alpha = 0.9588$ . The strain increases as cooking temperature or cooking time increases. Al dente samples (star symbols) reported higher strain compared to that of sample cooked at distilled water at the same temperature. (c) Young’s modulus measurement setup. Sample modulus is measured with DMA after every 3 min of cooking. (d) Experimental Young’s modulus data and analytical solution for the centroid of the modulus over time. Initial modulus is  $E_0 = 2.17$  GPa, and the modulus drops by five orders of magnitude after sufficient cooking. The error bars of the plots are the standard deviation of the average strain of three measurements. We use 0.8 wt. % salted water at 100 °C for Al dente (star symbols). Al dente samples (star symbols) reported higher modulus values compared to that of sample cooked at distilled water at the same temperature. The dashed gray lines separate the polymer regimes: the glassy regime (I), the leathery regime (II), and the rubbery regime (III). Regime II starts when the liquid concentration at the center of the cylinder starts to increase and ends when it reaches the maximum concentration possible before the polymer matrix relaxation starts. (e) Qualitative description of the modeling of the flexural rigidity of the pasta. (i) The spatial gradient of the elastic modulus in the pasta cross section, normal to the vertical axis. Liquid concentration within the pasta increases gradually, so the modulus gradient exists radially. (ii) Discretization of modulus gradient. To model the rigidity, we divided the pasta into 50 co-axial cylinders ( $N = 50$ ). Using the local modulus and the timely growth of the pasta radius, one can obtain the rigidity of each hollow co-axial cylinders:  $B_j = E_j l_j$  [Eq. (5)].

with the polymer matrix relaxation rate (see Note S1 for the detailed derivation). Next, we replace the length scale,  $\delta$ , with the radius of the pasta noodle as a function of time,  $r(t) = R[1 + \epsilon_r(t)]$ . Considering the swelling effects of pasta, we conclude the geometrical factors in the elastocapillary length to be  $I \sim (1+\epsilon)^4$  and  $p \sim (1+\epsilon)$ , so  $I/p \sim (1+\epsilon)^3$ .

To fit the model to the pasta swelling during cooking, the hygroscopic strain and elastic modulus of the pasta noodle at various cooking times and temperature were measured for 2 mm-diameter spaghettis (brand name De Cecco). In our experimental window—maximum of 30 min of cooking, spaghetti noodles display radial strain and axial strain approximately of 70% and 40%, respectively (see Note S3 for axial strain data). This difference is due to the difference in exposed surface area of pasta to the liquid where the stiffer inner region of the pasta interrupt elongation in the axial direction. The radius of the pasta at saturation was 96% of the initial, uncooked radius, for both the cooking temperatures, 80 °C and 100 °C. We observed that the presence of the salt ions in the water (Al dente recipe) facilitates hygroscopic swelling. We report  $D_0$  of 80 °C and 100 °C is  $D_0 = 3.6 \times 10^{-10} \text{ m}^2/\text{s}$  and  $D_0 = 6.3 \times 10^{-10} \text{ m}^2/\text{s}$ , respectively. Then, we compare our numerical modeling with the experimental measurements of radial expansion at various cooking times, as shown in Fig. 3(b).

Liquid migration into the pasta not only swells it but also causes significant softening. To obtain the quantitative trend of pasta softening, we measure the elastic modulus of the pasta in various cooking times by using the Dynamic Mechanical Analyzer (DMA-850, TA instrument's). We submerge the samples (noodles) in hot water and cook them for set cooking times, as shown in Fig. 3(c). The pasta is considerably rigid at an initial stage, but elastic modulus exponentially decreases as cooking time increases. Similar to what we observe in the modulus-temperature curve of polymers, we observe three regimes when we plot  $\log(E)$  vs time. In the regime I, equivalent to the hard-glassy region, the modulus drops very slowly. In regime II, where the glassy to rubbery transition occurs, the modulus quickly drops, three orders of magnitude within about 4 min. In regime III, the rubbery region, the modulus asymptotically reaches a final value for the fully cooked pasta. Unexpectedly, the presence of salt ions in the water stiffens the material compared to the modulus of the noodle cooked in the same condition but without salt. Overall, the modulus drops by five orders of magnitude from the initial ( $E_0 = 2.17 \text{ GPa} \pm 0.15$ ) to the saturated ( $E_s \sim 10^2 \text{ kPa}$ ) [see Fig. 3(d)]. Similar initial values of elastic modulus of pasta noodle were reported in previous work.<sup>31</sup>

To mathematically describe the elastic modulus variation with the cooking time (softening dynamics), we used the Weibull cumulative distribution function of the form (CDF),  $F(C; \eta, \theta) = 1 - \exp[-(C/\eta)^\theta]$ , where  $\eta$  and  $\theta$  are scale and shape parameters of the Weibull CDF, respectively. Weibull statistics have been traditionally used in mechanics to represent fracture problems where it describes how bond ruptures in the secondary bonds inside the polymer network lead to orders of magnitude drop in the modulus during the glassy to rubbery state transition.<sup>32,35</sup> Previously, this state in transition, so-called “reptation,” as de Gennes puts it,<sup>36</sup> would sometimes be modeled using Boltzmann distribution, where it only took in the bond rupture activation energy to estimate the modulus. However, we agree with the Mahieux and Reifsnider’s argument that the secondary bond rupture happens at different times “due to the distance variations

between atoms inducing a distribution in the strength of the interactions,” and hence adopt the Weibull statistics to model the modulus of the starch granules, which is a semi-crystalline polymer.<sup>37</sup> Using Weibull statistics for modeling modulus drop is, hence, also based on the relation between extreme swelling and bond rupture, but the details of these changes in molecular microstructure are outside the scope of this study.

Adopting Slade and Levine’s temperature and moisture content equivalency,<sup>38</sup> the Weibull modulus can be written as a function of liquid concentration within the pasta,<sup>30</sup>

$$E(r, t) = E_0 - [E_0 - E_s] \cdot \left[ 1 - \exp\left(-\left(\frac{C(r, t)}{\eta}\right)^\theta\right) \right], \quad (3)$$

where  $E_0$  and  $E_s$  correspond to the elastic modulus of the initial and saturation, respectively.  $E_0$  and  $E_s$  constrain the upper and lower boundary of the modulus in our experimental window and are experimentally obtained,  $E_0 = 2.17 \text{ GPa}$  and  $E_s = 50.8 \text{ kPa}$ , respectively. The local modulus in Eq. (3) is expressed as a function of local water concentration,  $C(r, t)$ . This model allows us to express the modulus of the pasta at any radial position at the varying hydration, thus plasticization, rate. Using existing models,<sup>12,35</sup> we can theoretically rationalize the elastic modulus variation with the water concentration. This expression can generally be used for finding the modulus of polymers swollen by liquid with spatial and time variation within the polymer matrix.

We can find  $\eta$  and  $\theta$  by comparing the area-averaged modulus to the experimentally measured modulus. By integrating Eq. (3) over the area, we obtain the area-average Young’s modulus:

$$E(t) = \frac{1}{\pi r(t)^2} \int_0^{2\pi} \int_0^R E(r, t) r dr d\theta. \quad (4)$$

Then, by fitting the centroid of the local modulus to the measured elastic modulus, one can back-solve for the parameters  $\eta$  and  $\theta$ . We report the  $\eta = 0.063$  and  $\theta = 1.0$ , same for both the cooking temperatures. The experimentally measured Young’s modulus of the composite and the Weibull-fitted expression of the modulus are drawn in Fig. 3(d) (see Note S2 for the detailed explanation for this parameters). Figure 3(d) shows regime boundaries as well. Gray lines divide the glassy regime (I), leathery regime (II), and the rubbery regime (III). We observed that the regime II starts when the liquid penetration reaches to the center of the pasta ( $\sim 8 \text{ min}$  for 100 °C cooking and  $\sim 14 \text{ min}$  for 80 °C cooking) and ends when the concentration at the center of the cylinder reaches the critical concentration,  $C^*$  ( $\sim 11 \text{ min}$  for 100 °C cooking and  $\sim 20 \text{ min}$  for 80 °C cooking).

Now that we have expressions for local elastic modulus and the radial strain, we can define the flexural rigidity of the pasta at any cooking time,  $B(t)$ , with the expressions found in Eqs. (2) and (3), as shown in Eq. (5),

$$B(t) = \frac{\pi}{4} \sum_{j=0}^N E_j(t) [r_{j+1}(t)^4 - r_j(t)^4]. \quad (5)$$

Here, the subscript  $j$  denotes the  $j$ th co-axial cylinder whose inner diameter equals  $r_j(t)$ , outer diameter equals  $r_{j+1}(t)$ , and the modulus equals  $E_j(t)$ , as illustrated in Fig. 3(e). We introduce this co-axial

discretization model to treat the pasta numerically as a multi-layered composite of gradually increasing softening from the core to the shell. The number of layers,  $N$ , is 50. Substituting the above expressions to the expression of  $l_{ec}$  gives the following expression of the stick length as a function of the measured parameters:

$$l_s \sim \left\{ d \left[ \frac{B(t)}{8 \gamma(T) \cdot r(t)} \right]^{1/2} \right\}^{1/2}. \quad (6)$$

We assume the liquid wets each half of the cylinder perimeter;<sup>22</sup> hence, the wicking perimeter  $p$  is  $2\pi r(t)$ . Furthermore, the surface tension of our cooking liquid, water, is assumed constant throughout the experiment; although the starch concentration in the water bath would gradually increase because the change in the concentration of starch in the water bath is very small ( $dC_{solute} \sim 0$ ), we assume a constant surface tension for each cooking temperature. For 80 °C, the surface tension of water is 62.67 mN/m, and for 100 °C, it is 58.91 mN/m.<sup>39</sup>

To validate our theoretical model, Eq. (6), we experimentally measured  $l_s$  in various cooking times, as shown in Fig. 4(a). The stick length experiments were done by submerging and then subsequently removing pasta noodle from a heated water bath conditioned at either 80 °C or 100 °C. Pasta noodles mounted at the top were cooked up to 30 min, and noodles were drained out of the bath at set cooking times (every 3 min) to measure the stick length. We plot the experimental data and the analytic solution for the stick length in Fig. 4(b). The pre-factor for the scaling law,  $\psi$ , is used to precisely fit the experimental results:  $l_s = \psi (dl_{ec})^{1/2}$ , where  $\psi = 1.15$ .

We observed that  $l_s$  initially drops exponentially until it reaches equilibrium. The capillary-induced adhesion starts during regime II of  $\log(E)$  vs time. Interestingly, even with an increment of the radius of pasta,  $l_s$  exponentially decreases at early cooking times. This is because the rigidity,  $B$ , is determined by not only the size of the structure but also the elastic modulus of it; in the case of pasta, the decrease in modulus is much larger than the increase in strain triple powered ( $l/p$ ) at early cooking times. This trend in  $l_s$  agrees with our expectation; because the modulus drops quickly initially,  $l_s$  decreases quickly at first, and it levels down eventually as cooking time increases. Hence,  $l_s$  is highly modulus dependent.

Adding salt in the cooking water, which many cooking books advise for better pasta texture, affects the chemical and mechanical properties of the pasta in some interesting ways. We observed increase in both the strain (swelling) and modulus (stiffening) of the noodles cooked in salted water compared to those cooked in distilled water, as shown in the star symbols of Figs. 3(b) and 3(d). Increase in the rate of hygroscopic swelling can be related to the facilitated transport of the “hydrated ions” into the polymer. Some studies reported increase in water/ion mobility into polymer matrix with increase in the salt concentration.<sup>40</sup> This would mean there would be less modulus gradient within the solid as water diffusion is faster with ions. Increase in the modulus is attributable to the increased van der Waals attraction induced by the presence of salt ions between the macromolecular chains. Thus, plasticization by hydration occurs slower. Our interpretation is that the addition of salt would provide more homogenous and unique texture due to ionic interaction.

Further commenting on the eating texture, we can relate the fracture properties of the cooked pasta to edibility. We can argue that our

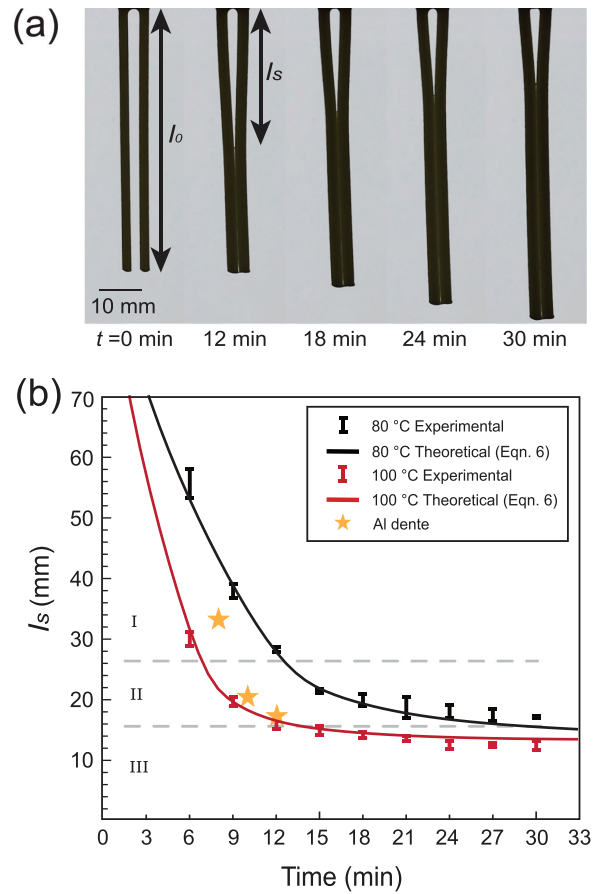


**FIG. 4.** (a) Pictures of pasta stiction over cooking time. Stick length decreases over time while radius and length of the pasta increase. (b) Experimental stick length data and analytical solution for the stick length over time. Stick length exponentially decreases until saturates. The error bars are the standard deviation of the average strain of three measurements. Stick length of Al dente samples increased compared to samples cooked at 100 °C without salt. It is mainly due to increased modulus [see Fig. 3(d)]. The dashed gray line separates the polymer regime: the glassy regime (I), the leathery regime (II), and the rubbery regime (III). Regime II starts when the liquid concentration at the center of the cylinder starts to increase and ends when it reaches the maximum concentration possible before the polymer matrix relaxation starts.

findings of the softening of pasta can effectively be used to infer edibility of the noodle. By introducing Griffith energy criteria, the stress required to create new surface through fracture can be expressed as  $\sigma \sim \sqrt{\gamma_p E/a}$ , where  $\gamma_p$  is the surface energy of the cooked pasta and  $a$  is an preexisting microcrack in the noodle. This stress, which scales with  $\sqrt{E}$ , hence clearly scales linearly also with the measured stick length  $l_s$ . Therefore, using the values reported in Fig. 3(d), we expect chefs can gauge the pasta texture without “eating.”

We were surprised to realize that within the few minutes cooking range of the al dente recipe recommended by various manufacturers, the modulus drops by two orders of magnitude. This necessitates great experience in cooks to taste the right texture of al dente and, as expected, causes great variation. We also now hypothesize that giving

a few-minute cooking range on most packages aims to accommodate the great sensitivity to the amount of added salt. On the other hand, our simple elastocapillarity experiment can accurately target a specific cooking time with a simple ruler measurement of the stick length between two hanging pasta noodles. Perhaps this experiment can further be validated by professional chefs, and one day used by home cooks.

In summary, we have studied the capillary-induced coalescence of swelling pasta. We observed that, as pasta is cooked (hence, swollen and softened), capillary action more easily deforms the noodle, and two pasta noodles can coalesce with the shorter stick length. Our predictive model that incorporates hygroscopic swelling and local elastic modulus as functions of the liquid concentration successfully captured the trend in the capillary coalescence of pasta. We believe that this work can provide insight to manufacturers for determining an optimal cooking time for the most delectable pasta texture.

## SUPPLEMENTARY MATERIAL

See the [supplementary material](#) document included online. It describes the solution to the diffusion equation and the swelling relation, modeling of the elastic modulus of cooked pasta, and the axial elongation of cooked pasta.

## ACKNOWLEDGMENTS

This work was supported by NSF CMMI (Grant No. 1825758).

## AUTHOR DECLARATIONS

### Conflict of Interest

The authors have no conflicts to disclose.

### Author Contributions

J. Ha and S. Tawfick conceived the idea for this article for the special issue Kitchen Flows. J. Hwang and J. Ha equally contributed to the experiments, modeling and writing. R. Siu and Y.S. Kim performed experiments. J. Hwang, J. Ha and S. Tawfick wrote the manuscript.

### DATA AVAILABILITY

The data that support the findings of this study are available within the article and its [supplementary material](#).

## REFERENCES

- N. N. Goldberg and O. M. O'Reilly, "Mechanics-based model for the cooking-induced deformation of spaghetti," *Phys. Rev. E* **101**, 013001 (2020).
- R. H. Heisser, V. P. Patil, N. Stoop, E. Villermaux, and J. Dunkel, "Controlling fracture cascades through twisting and quenching," *Proc. Natl. Acad. Sci. U. S. A.* **115**, 8665–8670 (2018).
- Y. Tao *et al.*, "Morphing pasta and beyond," *Sci. Adv.* **7**, eabf4098 (2021).
- K. Irie, A. K. Horigane, S. Naito, H. Motoi, and M. Yoshida, "Moisture distribution and texture of various types of cooked spaghetti," *Cereal Chem.* **81**, 350–355 (2004).
- J. E. Dexter, R. H. Kilborn, B. C. Morgan, and R. R. Matsuo, "Grain research laboratory compression tester: Instrumental measurement of cooked spaghetti stickiness," *Cereal Chem.* **60**, 139–142 (1983).
- J. J. Gonzalez, K. L. McCarthy, and M. J. McCarthy, "Textural and structural changes in lasagna after cooking," *J. Texture Stud.* **31**, 93–108 (2000).
- R. Jumaidin *et al.*, "Water transport and physical properties of sugarcane bagasse fibre reinforced thermoplastic potato starch biocomposite," *J. Adv. Res. Fluid Mech. Therm. Sci.* **61**, 273–281 (2019).
- N. Soykeabkaew, C. Thanomsilp, and O. Suwantong, "A review: Starch-based composite foams," *Composites, Part A* **78**, 246–263 (2015).
- M. Gáspár, Z. Benko, G. Dogossy, K. Réczey, and T. Czigány, "Reducing water absorption in compostable starch-based plastics," *Polym. Degrad. Stab.* **90**, 563–569 (2005).
- C. Cunin, S. Handschin, P. Walther, and F. Escher, "Structural changes of starch during cooking of durum wheat pasta," *LWT—Food Sci. Technol.* **28**, 323–328 (1995).
- T. Van Vliet and P. Walstra, "Large deformation and fracture behaviour of gels," *Faraday Discuss.* **101**, 359–370 (1995).
- W. Weibull, "A statistical distribution function of wide applicability," *J. Appl. Mech.* **18**, 293–297 (1951).
- H. Bense *et al.*, "Elastocapillary adhesion of a soft cap on a rigid sphere," *Soft Matter* **16**, 1961–1966 (2020).
- J. Bico, É. Reyssat, and B. Roman, "Elastocapillarity: When surface tension deforms elastic solids," *Annu. Rev. Fluid Mech.* **50**, 629–659 (2018).
- H.-Y. Kim and L. Mahadevan, "Capillary rise between elastic sheets," *J. Fluid Mech.* **548**, 141–150 (2006).
- J. Bico, B. Roman, L. Moulin, and A. Boudaoud, "Elastocapillary coalescence in wet hair," *Nature* **432**, 690 (2004).
- Z. Wei, T. M. Schneider, J. Kim, H.-Y. Kim, J. Aizenberg, and L. Mahadevan, "Elastocapillary coalescence of plates and pillars," *Proc. R. Soc. A Math. Phys. Eng. Sci.* **471**, 2175 (2015).
- J. Ha, Y. S. Kim, K. Jiang, R. Siu, and S. Tawfick, "Hydrodynamic elastocapillary morphing of hair bundles," *Phys. Rev. Lett.* **125**, 254503 (2020).
- D. Shin and S. Tawfick, "Polymorphic elastocapillarity: Kinetically reconfigurable self-assembly of hair bundles by varying the drain rate," *Langmuir* **34**, 6231–6236 (2018).
- C. Duprat, J. M. Aristoff, and H. A. Stone, "Dynamics of elastocapillary rise," *J. Fluid Mech.* **679**, 641–654 (2011).
- J. M. Aristoff, C. Duprat, and H. A. Stone, "Elastocapillary imbibition," *Int. J. Non. Linear. Mech.* **46**, 648–656 (2011).
- A. E. Cohen and L. Mahadevan, "Kinks, rings, and rackets in filamentous structures," *Proc. Natl. Acad. Sci. U. S. A.* **100**, 12141–12146 (2003).
- P.-G. de Gennes, F. Brochard-Wyart, and D. Quéré, *Capillarity and Wetting Phenomena* (Springer, 2004).
- J. Yoon, S. Cai, Z. Suo, and R. C. Hayward, "Poroelastic swelling kinetics of thin hydrogel layers: Comparison of theory and experiment," *Soft Matter* **6**, 6004–6012 (2010).
- J. Ha and H.-Y. Kim, "Capillarity in soft porous solids," *Annu. Rev. Fluid Mech.* **52**, 263–284 (2020).
- T. Bertrand, J. Peixinho, S. Mukhopadhyay, and C. W. MacMinn, "Dynamics of swelling and drying in a spherical gel," *Phys. Rev. Appl.* **6**, 064010 (2016).
- M. Tokita and T. Tanaka, "Friction coefficient of polymer networks of gels," *J. Chem. Phys.* **95**, 4613–4619 (1991).
- C. Allain and C. Amiel, "Permeability measurements during the sol-gel transition: Direct determination of the exponent  $\nu$ ," *Phys. Rev. Lett.* **56**(14), 1501 (1986).
- F. A. Long and D. Richman, "Concentration gradients for diffusion of vapors in glassy polymers and their relation to time dependent diffusion phenomena," *J. Am. Chem. Soc.* **82**, 513–519 (1960).
- S. Cafieri, M. Mastromatteo, S. Chillo, and M. A. Del Nobile, "Modeling the mechanical properties of pasta cooked at different times," *J. Food Eng.* **100**, 336–342 (2010).
- F. Akbar and M. Abdullah, "Using hot steam exposure to reveal mechanical properties of spaghetti beams and columns," *J. Food Sci.* **86**, 1672–1680 (2021).
- C. A. Mahieux and K. L. Reifsnider, "Property modeling across transition temperatures in polymers: Application to thermoplastic systems," *J. Mater. Sci.* **37**, 911–920 (2002).
- M. A. Del Nobile, G. G. Buonocore, A. Panizza, and G. Gambacorta, "Modeling the spaghetti hydration kinetics during cooking and overcooking," *J. Food Sci.* **68**, 1316 (2003).

- <sup>34</sup>S. Cafieri, S. Chillo, M. Mastromatteo, N. Suriano, and M. A. Del Nobile, “A mathematical model to predict the effect of shape on pasta hydration kinetic during cooking and overcooking,” *J. Cereal Sci.* **48**, 857–862 (2008).
- <sup>35</sup>J. Richeton, G. Schlatter, K. S. Vecchio, Y. Rémond, and S. Ahzi, “A unified model for stiffness modulus of amorphous polymers across transition temperatures and strain rates,” *Polymer* **46**, 8194–8201 (2005).
- <sup>36</sup>P. G. de Gennes, *Scaling Concepts in Polymer Physics* (Cornell University Press, 1979).
- <sup>37</sup>E. Bertoft, “Understanding starch structure: Recent progress,” *Agronomy* **7**, 56 (2017).
- <sup>38</sup>L. Slade and H. Levine, “Water and the glass transition—Dependence of the glass transition on composition and chemical structure: Special implications for flour functionality in cookie baking,” *J. Food Eng.* **22**, 143–188 (1994).
- <sup>39</sup>N. B. Vargaftik, B. N. Volkov, and L. D. Voljak, “International tables of the surface tension of water,” *J. Phys. Chem. Ref. Data* **12**, 817–820 (1983).
- <sup>40</sup>R. Zhang, Y. Zhang, H. S. Antila, J. L. Lutkenhaus, and M. Sammalkorpi, “Role of salt and water in the plasticization of PDAC/PSS polyelectrolyte assemblies,” *J. Phys. Chem. B* **121**, 322–333 (2017).